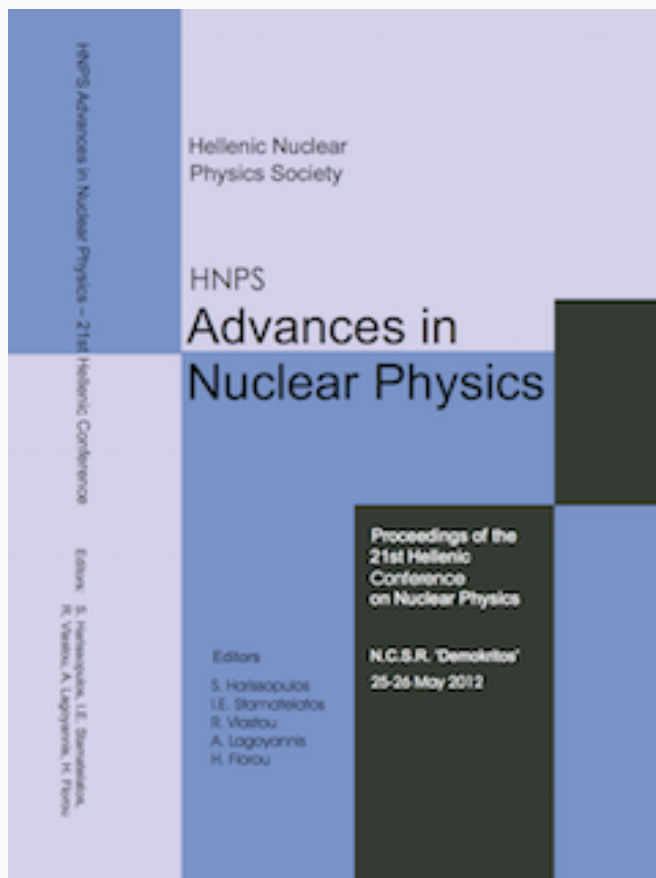


HNPS Advances in Nuclear Physics

Vol 20 (2012)

HNPS2012



Phantom Experimentation on SPECT, Infrared and Optical Tomography

A.-N. Rapsomanikis, M. Kontos, J. Menis, M. Mikeli, M. Zioga, E. Stiliaris

doi: [10.12681/hnps.2489](https://doi.org/10.12681/hnps.2489)

To cite this article:

Rapsomanikis, A.-N., Kontos, M., Menis, J., Mikeli, M., Zioga, M., & Stiliaris, E. (2012). Phantom Experimentation on SPECT, Infrared and Optical Tomography. *HNPS Advances in Nuclear Physics*, 20, 66–72.

<https://doi.org/10.12681/hnps.2489>

Phantom Experimentation on SPECT, Infrared and Optical Tomography

A.-N. Rapsomanikis^a, M. Kontos^b, J. Menis^a, M. Mikeli^a,
M. Zioga^a and E. Stiliaris^{a,c 1}

^a*Department of Physics, National & Kapodistrian University of Athens, Athens, Greece*

^b*LAIKO General Hospital, Medical School, National and Kapodistrian University of Athens, Athens, Greece*

^c*Institute of Accelerating Systems & Applications (IASA), Athens, Greece*

Abstract

The Single Photon Emission Computed Tomography (SPECT) using simple γ -radiotracers has been established as a standard technique in the physiological and functional nuclear imaging. On the other hand, accurate reconstruction of abnormalities inside biological tissues based on the detected temperature distribution obtained at the surface of the skin presents a major challenge in emission thermography. The present work focuses on the experimental study with these modalities using appropriately constructed ^{99}Tc and thermal phantoms. Special emphasis was given to the relationship between the physical characteristics, such as the location and the emission power of an embedded heat source inside an absorbing medium and the measured temperature distribution by means of infrared imaging. Those thermal phantoms were studied at temperature $35^{\circ} - 40^{\circ}\text{C}$, which corresponds to mammal's core temperature. The obtained planar information was further analyzed to reconstruct the tomographic images, and from them, the final 3D image of the phantoms. The reconstruction procedure was performed with iterative algorithms based on MLEM and accelerated ART techniques. In order to investigate scattering and absorption effects, the same reconstruction procedure has been applied to optical (fluorescence) tomography with appropriately constructed phantoms. Reconstructions results are presented in this study for different phantom depth locations and heat generation rates.

Key words: SPECT, Infrared Tomography, Optical Tomography, Emission Phantoms, Image Reconstruction Algorithms, MLEM, ART

¹ Corresponding author: stiliaris@phys.uoa.gr

1 Introduction

SPECT is unambiguously a powerful, low cost diagnostic technique in modern medical practice. Nonetheless, one of its major drawbacks arises from the nature of the detected ionizing radiation, which makes difficult to obtain the anatomical information of the area under investigation without the assistance of another modality (X-Ray CT, MRI). The extra load of ionizing radiation (CT), the high cost (MRI) and also the mobility of such devices make those methods superfluous. Our SPECT-Lab has recently developed and evaluated on a tomographic level, a small-field γ -Camera system based on Position Sensitive PhotoMultiplier Tubes (PSPMT) [1]. Therefore, in order to gain the necessary anatomic information two different, non invasive, non-ionizing, low cost and portable modalities are proposed in the current project. These are the Optical and Thermal Computed Tomography, both in emission processes.

It is well known that a thermal or infrared emission imaging procedure measuring the temperature distribution on the surface of a live organism can potentially indicate abnormalities inside the biological tissue. The great advantage of this technique is the absence of any radioactive or ionizing tracers and the utilization of the body's own thermal radiation. Nevertheless, one of the most cited drawbacks of this modality is the absence of standard procedures which can dynamically correlate the obtained information to the physical characteristics, such as the exact location and the heat emission of the source.

The main goal of the present study is to experimentally define the capabilities of the infrared emission tomography at the scale of mammal's core temperatures, as well as the optical tomography fluorescence light emission, by means of appropriate phantom experimentation. This will also serve as a feasibility study in the design of a dual-modality imaging system with the existing portable γ -Camera system of our Lab [1] by incorporating a future infrared and optical tomography additionally to the existing SPECT option. Therefore, the tasks posed in this study require a reasonable selection of the appropriate phantoms and imaging conditions, as well as an efficient reconstruction technique.

2 Experimental Results

2.1 SPECT Modality

The SPECT modality has already been tested both on planar and tomographic level [1] by constructing an axially asymmetrical phantom consisting of three

different cylindro-conoidal tubes and two capillaries, filled with ^{99m}Tc solution of special concentration 0.25 mCi/ml. In addition, absorption was introduced by immersing the phantom in agarose gel. The obtained spatial resolution was on planar $\langle \sigma_x \rangle = (0.95 \pm 0.05)$ mm, $\langle \sigma_y \rangle = (1.07 \pm 0.07)$ mm. Similarly, on the tomographic level the spatial resolution was determined to be in the order of 2 mm in X- and Y-Axis, with the smallest detectable object the capillaries volume (0.073 cm^3) for the given special activity, as shown in Figure 1.

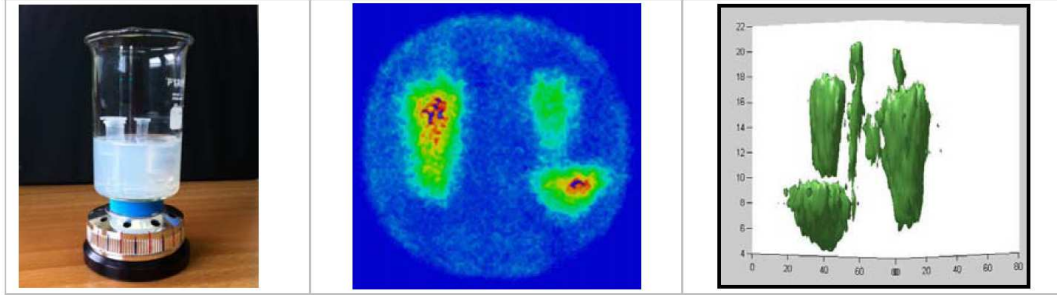


Fig. 1. *Left:* A picture of the examined phantom. *Middle:* One of the planar images obtained by the γ -Camera system. *Right:* The final 3D-reconstructed image.

2.2 Infrared Modality

A phantom capable of emitting thermal radiation was constructed out of six resistances (100Ω and 50Ω) of the same volume grouped in three pairs and alternately connected in series, in order to manipulate their temperature. They were morphed to shape the capital letter **M**, leaving the middle pair of resistors out of plane (Figure 2, Upper Part). The selected temperature scale was mammal's core temperatures ($35^{\circ} - 40^{\circ} \text{ C}$) since the goal of this study is to study the properties of such a system toward to a clinical application.

In order to introduce absorption to the system, as a more realistic case scenario, the same phantom, after tested in a absorption free environment, was immersed in agarose gel (Figure 2, Lower Part) of 1gr/100ml concentration with nearly water density. Because the gel environment was cold the temperature of the phantom was raised above the core temperature of mammals (49.5° C) as an attempt to keep the relative temperature closer to the principle range.

The phantom was placed on a small rotating platform, thus the thermal camera has remain fixed and a total of 24 projections, covering the full 360° -range in steady steps of 15° , were accumulated. The thermal fingerprint of the infrared phantom in both cases of absorbing and non-absorbing environment has been detected by a portable thermal camera (Thermovision 550, AGEMA Infrared Systems AB) [2] with a built-in 200 lens in the form of high resolution



Fig. 2. *Upper Part:* The thermal phantom used in this study placed on a rotating table. It consists of six resistors connected in series. Phantom dimensions: $50\text{ mm} \times 50\text{ mm} \times 15\text{ mm}$. *Lower Part:* The thermal phantom incased in agarose gel environment (1gr/100ml concentration) Phantom dimensions: $100\text{ mm} \times 70\text{ mm} \times 60\text{ mm}$.

color images (250x188 pixels) (Figure 3). Finally, all the planar information was obtained by calibrating the camera for the same exposure and other necessary set-ups.

Every of the 24 projections was axially sliced (slice width=1.5 mm) after taking into account different offsets in order to reduce the background noise. Then, by using our own algorithms, based on the accelerated ART and MLEM techniques [3], the tomographic images were reconstructed. Thereby, the capability of reconstructing on infrared without utilizing any absorption correction method, for both absorption and absorption-free cases, has been successfully tested. Planar images are visualized after the tomographic processing with the aid of the MathCAD package.

All the tomographic images were then isosurface plotted by using the MATLAB package in order to create the final 3D images of the phantom. A typical 3D-reconstruction result is shown in Figure 4 for both, non-absorbing and absorbing thermal emission.

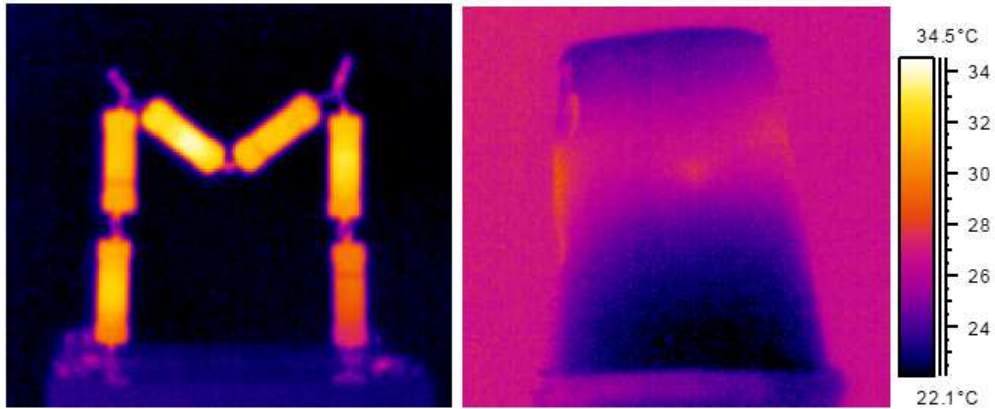


Fig. 3. *Left*: Planar images (no absorbing medium) obtained with the thermal camera. *Right*: Planar images obtained in the agarose absorbing medium with the thermal camera. The different colors depicted in the images indicate different temperatures emitted by the phantom. The fact that the emitted infrared radiation is a function of the phantom's surface temperature makes it possible for the camera to calculate those temperatures.

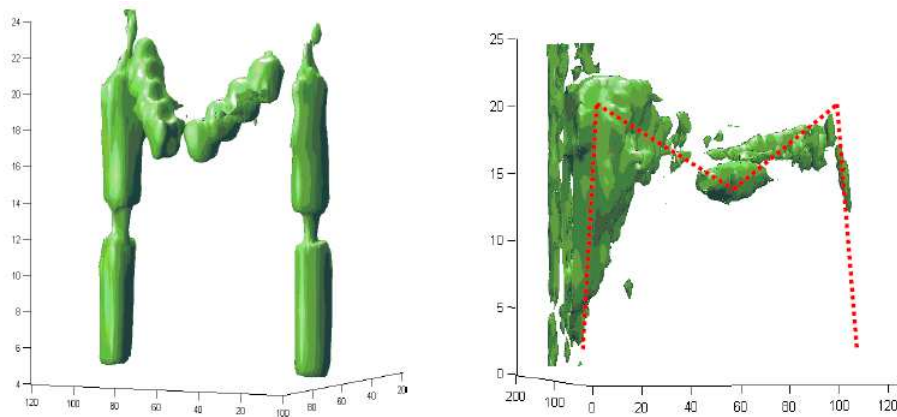


Fig. 4. *Left*: 3D reconstruction (ISO-Value=0.19) for a temperature of 36.5°C corresponding to a resistor current of $I = 40\text{ mA}$ (non absorbing medium). *Right*: 3D reconstruction (ISO-Value=0.07) for a temperature of 49.5°C corresponding to a resistor current of $I = 80\text{ mA}$ (agarose absorbing medium). The images were created by contour plotting all the obtained tomograms of the reconstruction process using the MATLAB package.

2.3 Optical Modality

In order to investigate the optical case, also a proper optical phantom capable of emitting in visible light was created. The phantom was consisting of three capillaries creating a pyramid formation and two cylidro-conoidal tubes, the one of which is placed off axis. They were all filled with fluorescent liquid (Cyalume) (Figure 5, Upper Part).

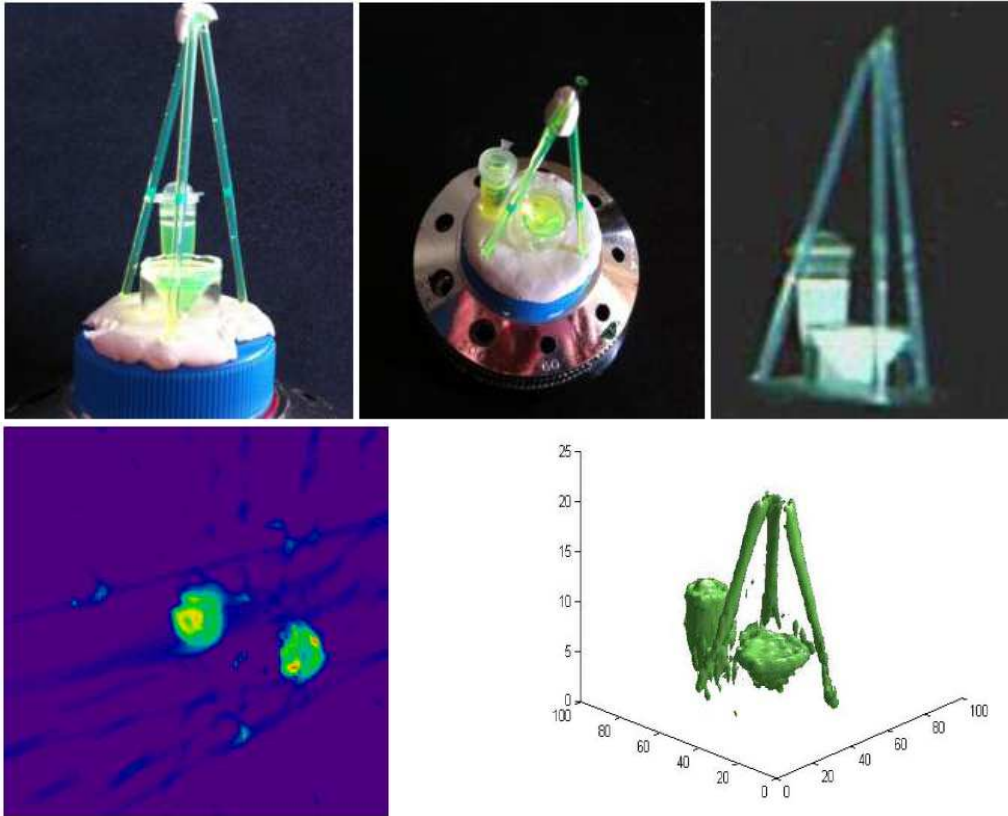


Fig. 5. *Upper Left and Middle:* The optical phantom used in this study from two different angles. It consists of three capillaries creating a pyramid formation and two cylindro-conoidal tubes, the one of which is placed off axis. They were all filled with fluorescent liquid (Cyalume). *Upper Right:* Planar image of the phantom obtained in the visual spectrum by a CCD camera. *Lower Left:* Tomogram of the optical phantom at level 3, visualized with the MathCAD package. *Lower Right:* 3D-reconstruction image (ISO-Value=0.14) created by contour plotting all the obtained tomograms using the MATLAB package.

The process of acquiring the planar images for the optical case was similar to the previous one followed in the infrared procedure. The planar images were obtained by a commercial CCD camera (American Dynamics) able to detect optical photons. Also, in order to reduce the background noise created by the ambient light, the whole construction was placed and photographed at a dark environment inside a dark box.

After obtaining the 24 projections the same reconstructing procedure was followed step by step for the optical phantom creating the tomograms and 3D reconstructed image (Figure 5, Lower Part).

3 Concluding Remarks

The capability of reconstruction by commonly used algorithms was investigated by means of emission phantom experimentation for physical procedures such as scattering and adsorption of thermal but also optical radiation. Both procedures are highly diffusive and the first results are promising towards adding two new modalities to the existing γ -Camera system operating in SPECT modality. The integrated system is going to be used in a clinical environment.

References

- [1] D. Thanasas *et al.*: *A correction method of the spatial distortion in planar images from γ -Camera systems*, Journal of Instrumentation **4** (2009) P06012.
- [2] AGEMA Infrared Systems: *Thermovision 550, Operating Manual*, Publ. Num. 557, 2007.
- [3] S. Angeli and E. Stiliaris: *An Accelerated Algebraic Reconstruction Technique based on the Newton-Raphson Scheme*, IEEE NSS-MIC Record M09-323 (2009) 3382-3387.